Spatio-Temporal Analysis of Future Precipitation Changes in the Huaihe River Basin Based on NEX-GDDP-CMIP6 Dataset and Monitoring Data

Min Tong , Leilei Li * , Zhi Li , Zhihui Tian

Posted Date: 13 September 2023

doi: 10.20944/preprints202309.0809.v1

Keywords: NEX-GDDP-CMIP6; extreme precipitation; climate change; Huaihe River Basin

Article

Spatio-Temporal Analysis of Future Precipitation Changes in the Huaihe River Basin Based on NEX-GDDP-CMIP6 Dataset and Monitoring Data

Min Tong [1], Leilei Li [2,*], Zhi Li [3,4] and Zhihui Tian [5]

[1] School of Earth Science and Technology, Zhengzhou University, Zhengzhou 450000,China; tongmin@gs.zzu.edu.cn
[2] School of Earth Science and Technology, Zhengzhou University, Zhengzhou 450000,China; stonejdx@zzu.edu.cn
[3] China Center for Resources Satellite Data and Application, Beijing 100094, China; lizhi@lreis.ac.cn
[4] China Siwei Surveying and Mapping Technology Co.Ltd, Beijing 100086, China; lizhi@lreis.ac.cn
[5] School of Earth Science and Technology, Zhengzhou University, Zhengzhou 450000,China; iezhtian@zzu.edu.cn
* Correspondence: stonejdx@zzu.edu.cn; Tel.: +86-18911719037

Abstract: This research analyses extreme precipitation events in the Huaihe River Basin in China, a densely populated region with a history of human settlements and agricultural activities. This study aims to explore the impact of extreme precipitation index changes and provide decision-making suggestions for flood early warning and agricultural development in the Huaihe River Basin. The study utilises the NEX-GDDP-CMIP6 climate models dataset and the daily value dataset (V3.0) from China's national surface weather stations to investigate temporal and spatial changes in extreme precipitation indices from 1960 to 2014 and future projections. At the same time, this study adopted the RclimDex model, Taylor diagram and Sen+Mann-Kendall trend analysis research methods to analyse the data. The results reveal a slight increase in extreme precipitation indices from northwest to southeast within the basin, except for CDD, which shows a decreasing trend. Regarding spatial, the future increase of extreme precipitation in the Huaihe River Basin will show a spatial variation characteristic that decreases from northwest to southeast. These findings suggest that extreme precipitation events are intensifying in the region. Understanding these trends and their implications is vital for adaptation strategy planning and mitigating the risks associated with extreme precipitation events in the Huaihe River Basin.

Keywords: NEX-GDDP-CMIP6; extreme precipitation; climate change; Huaihe River Basin

1. Introduction

In the past 100 years, the global climate has experienced changes characterized by warming. Extreme weather and climate events are more likely to occur on a global and regional scale, which have substantially negatively impacted ecosystems [1]. The Green Paper on Climate Change highlights that China is one of the regions notably influenced by climate change. Since the mid-20th century, the rate of temperature increase has exhibited a markedly elevated trajectory compared to the global average for the corresponding temporal span [2]. The harmful consequences of climate change in China predominantly outweigh any potential benefits [3]. Therefore, studying the potential changes in the extreme precipitation index due to future climate change is of great scientific significance for implementing corresponding mitigation and adaptation measures in the study area.

Severe precipitation events substantially influence human safety, socio-economic advancement and the integrity of natural ecosystems [4,5]. The frequency and intensity of extreme precipitation events in China and worldwide are increasing with global warming [6,7]. The IPCC Sixth Assessment Report pointed out that every 1 °C increase in global temperature in the future, the intensity of extreme daily precipitation events will increase by 7% [8]. Furthermore, the power of regional extreme precipitation has a nearly linear relationship with the extent of global warming. The greater

 doi:10.20944/preprints202309.0809.v1

the degree of global warming in the future, the more significant the increase in heavy precipitation. The Huaihe River Basin is prone to intense and continuous rainfall events, which lead to severe flood disasters. Accurate identification of temporal and spatial variation characteristics has become the focus of global attention [9].

Historically, the Huaihe River Basin has experienced frequent and severe extreme climate events. According to statistics, there were 979 floods in the Huaihe River Basin between 246 BC and 1948. Particularly during the 754 years following the Yellow River's capture of the Huaihe River (1194-1948), the region witnessed a staggering 594 significant flood events, translating to an average of 79 catastrophic inundations every century [10]. 1954, 1991 and 2003 were the three years with abnormal precipitation in the Huaihe River Basin since the founding of the People's Republic of China [11]. In the summer of 2007, the Huaihe River Basin faced historically unprecedented flood disasters, with many major cities and regions enduring sporadic torrential downpours, leading to a complex disaster scenario [12]. Since early July 2021, Henan Province has faced severe disasters that are rare in history. Especially on July 20, Zhengzhou city suffered heavy rain and severe floods that caused heavy casualties and property losses. Hence, policymakers and the general populace must comprehend extreme precipitation's temporal and spatial evolutionary traits within the Huaihe River Basin. A sophisticated analysis of the long-term extreme precipitation index proves instrumental in enhancing disaster prevention and mitigation strategies.

Currently, climate models are widely used for extreme precipitation simulations and future predictions. The new round of the International Coupled Model Intercomparison Project (CMIP6) released the output results of atmospheric circulation models developed by more than 30 institutions around the world, providing strong support for improving the accuracy of climate change predictions in the Huaihe River Basin [13]. Huang Xiaoyuan first selected five CMIP6 models with complete data based on previous achievements and used the bilinear interpolation method to uniformly interpolate data with different resolutions to a grid of 0.5°×0.5° for research [14]. To investigate the anticipated alterations in the characteristics of extreme precipitation in Guizhou Province due to climatic shifts, Feng Yelin conducted a comprehensive analysis of four distinct extreme precipitation indices at a spatial resolution of 0.5°×0.5°, utilizing station-based observations in conjunction with daily precipitation datasets derived from five CMIP6 models [15]. This study delves into the spatiotemporal dynamics of both historical and prospective changes. The data derived from the CMIP6 simulations employed in the aforementioned research exhibits a relatively low spatial and temporal resolution. When studying regions with rapidly changing environmental conditions, they cannot capture the local variability and nuances existing in the area. Therefore, they are unsuitable for extreme rainfall spatiotemporal changes that require fine-grained spatial information. For this reason, this paper uses high-resolution NEX-GDDP-CMIP6 experimental data for research, which provides essential support.

Natural disasters are frequent in the Huaihe River Basin and model resolution is an essential factor affecting the performance of precipitation simulation. Drawing upon the comprehensive datasets from 45 meteorological stations spanning the years from 1960 to 2014, this research meticulously selected and computed the pertinent extreme precipitation indices, analyzing the spatiotemporal variation characteristics of the Huaihe River Basin in the historical period (1960-2014). Afterwards, we construct the Taylor diagram to visually evaluate the performance of multiple high-resolution NEX-GDDP-CMIP6 climate models in simulating the Huaihe River Basin precipitation, select the top five models with the best performance averaging, calculate the extreme precipitation index and analyze its spatiotemporal changes feature in the future period (2015-2100). It explores the impact of extreme precipitation indices on the precipitation changes to provide decision-making suggestions for flood warnings and agricultural development in the Huaihe River Basin.

Preprints (www.preprints.org) | NOT PEER-REVIEWED | Posted: 13 September 2023 doi:10.20944/preprints202309.0809.v1

Materials and Methods

2.1. Study Area

The Huaihe River Basin is between the Yangtze River and the Yellow River in the eastern part of China. The geographical coordinates demarcate a region spanning from 111°55' to 121°25' in eastern longitude and encompassing 30°55' to 36°36' in northern latitude. The basin, originating from the western terrains of Tongbai and Funiu Mountains, extends its boundaries to the eastern periphery of the Yellow Sea. To the south, it delineates its contours along the Yangtze River, complemented by the majestic Dabie Mountains, the undulating Jianghuai Hills, the intricate waterways of the Tongyang Canal and the southern embankments of the Rutai Canal. Furthermore, its northern frontier is demarcated by the southern embankment of the Yellow River and the eminent Mount Tai, seamlessly adjoining the Yellow River Basin.

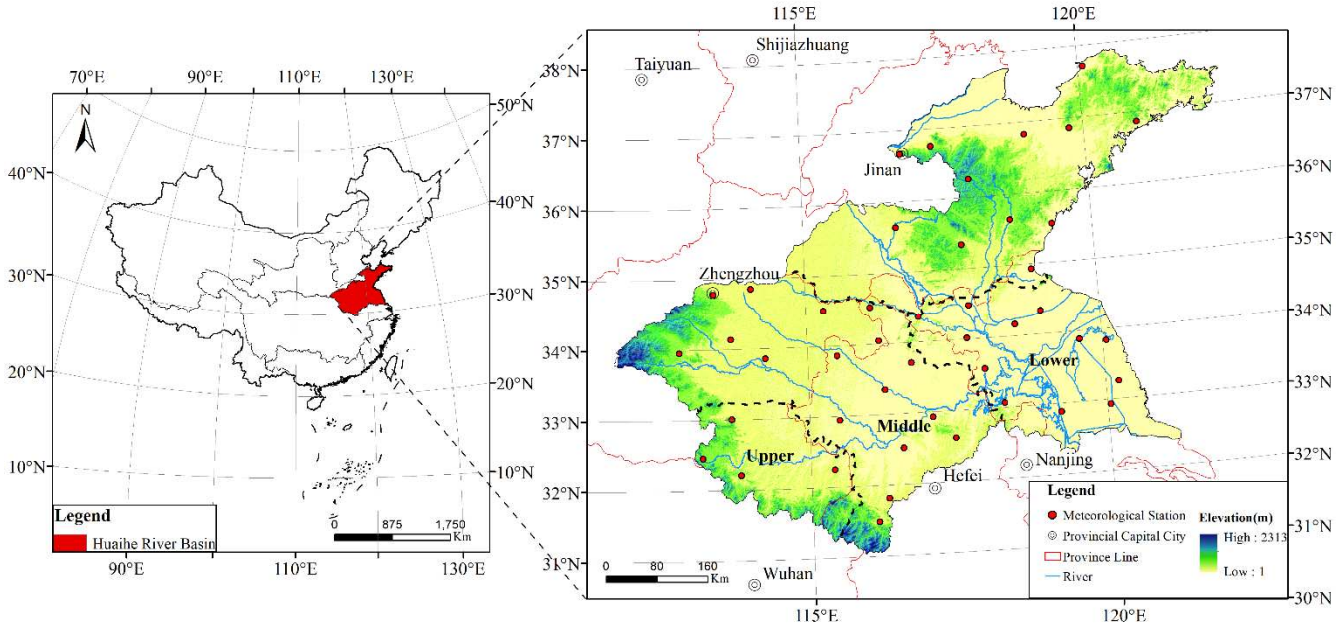

Figure 1. The spatial distribution of the Huaihe River Basin.

The Huaihe River Basin is in the transition zone from a subtropical humid climate to a warm temperate semi-humid climate. Due to the superimposed influence of multiple weather systems, the regional environment is changeable and the weather changes drastically, leading to uneven spatiotemporal rainfall distribution [16,17]. It has prominent seasonal characteristics, with high temperature and rain in summer and low temperature and little rain in winter. The annual average precipitation is between 572.6 and 1278.8 mm in the basin. In the Huaihe River Basin, the precipitation is predominantly concentrated during the flood season, spanning from May to September, which accounts for approximately 63.8% of the annual precipitation. This pattern underscores a pronounced spatiotemporal heterogeneity in the annual precipitation distribution, a phenomenon observed in various river basins across China [18]. Most rainfall focuses on the primary flood season and the basin's southern part. Extreme precipitation or long-term continuous precipitation can easily cause flood disasters, which belong to the flood-prone area.

2.2. Data Source

This investigation predominantly employs two distinct categories of data: the first encompasses historically recorded climatic measurements, while the second derives from future climatic projections sourced from NEX-GDDP-CMIP6.

Preprints (www.preprints.org) | NOT PEER-REVIEWED | Posted: 13 September 2023 doi:10.20944/preprints202309.0809.v1

2.2.1. Historically measured climate data

This study's historical measured climate data comes from the daily dataset (V3.0) of China's national surface meteorological stations. The daily observation data of critical meteorological factors on the ground since January 1951, including the daily precipitation of 45 meteorological stations in the Huaihe River Basin, are distributed in Zhengzhou, Kaifeng, Baofeng, Xuchang, Xihua, Zhumadian, Xinyang, Tongbai, Shangqiu, Gushi, Longkou, Haiyang, Pingdu, Weifang, Rizhao, Jinan, Zhangqiu, Yiyuan, Juxian, Feixian, Yanzhou, Dangshan, Yongcheng, Bozhou, Fuyang, Huoshan, Luan, Shouxian, Dingyuan, Bengbu, Mengcheng, Suzhou, Xuzhou, Pizhou, Ganyu, Guanyun, Shuyang, Suining, Sihong, Xuyi, Gaoyou, Funing, Sheyang, Dafeng and Dongtai. The period unifies to 1960-2014 (Figure 2).

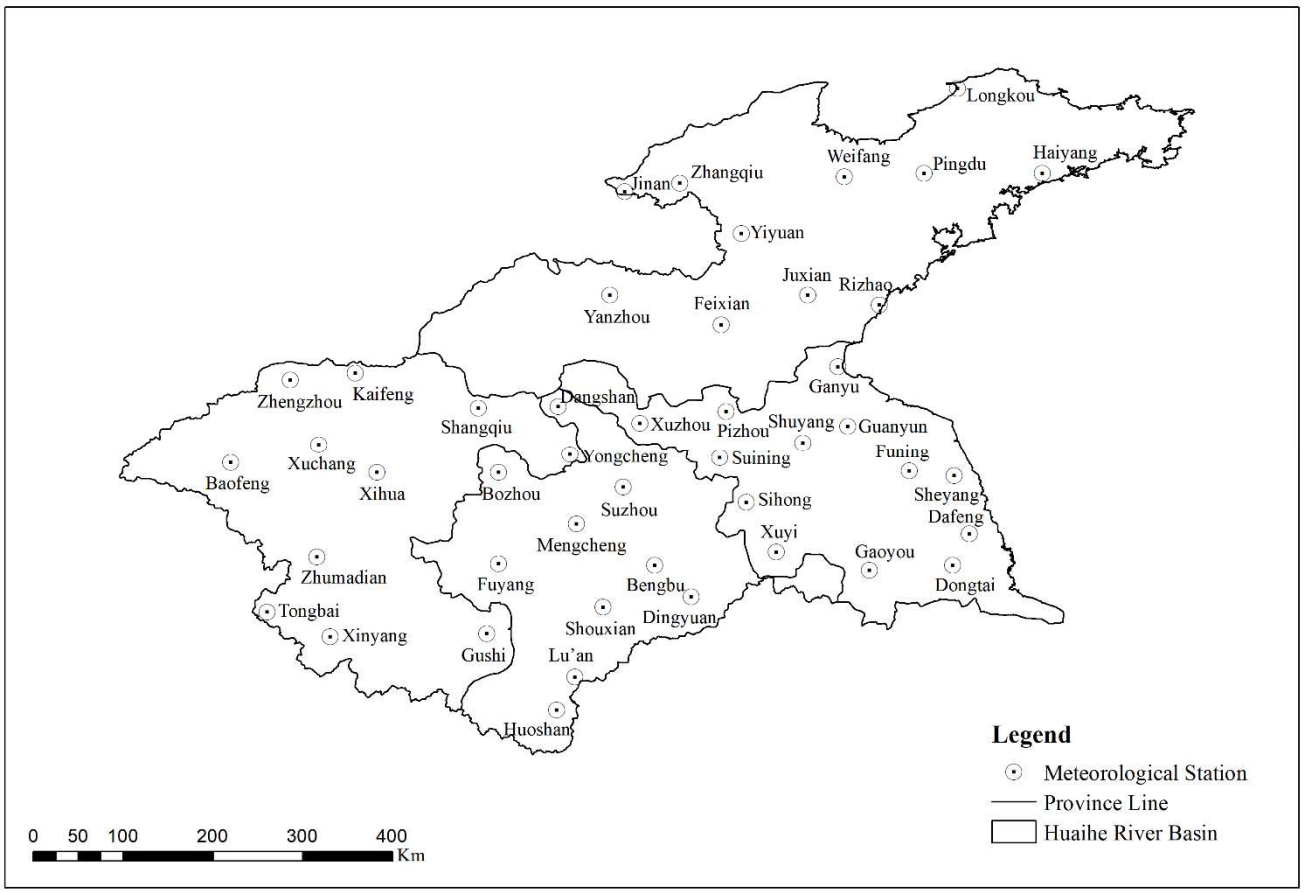

Figure 2. Distribution of 45 meteorological stations in the Huaihe River Basin.

2.2.2. NEX-GDDP-CMIP6 Dataset

The NEX-GDDP-CMIP6 dataset is a paramount asset for the scientific community, encompassing a sophisticated conversion mechanism that metamorphoses 35 CMIP6 precipitation data nodes into a streamlined resolution of precisely 0.25° by 0.25°. The process of 'downscaling' actualizes this intricate transformation, facilitating a superior granular spatial resolution.

The dataset encompasses not only historical data spanning 1950 to 2014 but also integrates data from four prospective scenarios. The Shared Socioeconomic Pathways (SSPs) scenarios define diverse trajectories of socioeconomic evolution that influence potential future climates. We designate these pathways as SSP1-2.6, SSP2-4.5, SSP3-7.0 and SSP5-8.5. Each pathway aligns with a distinct greenhouse gas concentration trajectory, with the subsequent number after the SSPs signifying the radiative forcing level anticipated by the century's conclusion.

We then use the data from these scenarios to make extreme precipitation index analysis covering the period from 2015 to 2100. This forecast period allows researchers to analyze and predict the

 doi:10.20944/preprints202309.0809.v1

potential impacts of various climate change scenarios. Therefore, the NEX-GDDP-CMIP6 dataset is an essential tool for climatologists to model possible future climate conditions and their effects.

We choose 13 models in this dataset, using 'r1i1p1f1' as the driver and 'gn' as the grid. The term 'r1i1p1f1' specifies the specific model run, initialization method, physics version and forcing used in each model, while 'gn' refers to the grid used for the model output. Integrating these sophisticated models, coupled with the distinct driver and grid infrastructure, provides a thorough and nuanced examination of climate data. The detailed specifics of each model, the driver, the grid and other essential information are neatly displayed in Table 1. By using this methodology, scholars can expediently cross-reference and incorporate the data into their empirical analyses, rendering the NEX-GDDP-CMIP6 dataset an indispensable cornerstone in climatological research.

Table 1. List of GCMs from CMIP6 project considered in this study.

Number	Model	Institution	Country	Resolution
1	ACCESS-CM2	ACCESS	Australia	0.25°×0.25°
2	ACCESS-ESM1-5	ACCESS	Australia	0.25°×0.25°
3	BCC-CSM2-MR	BBC	China	0.25°×0.25°
4	CMCC-CM2-SR5	CMCC	Italy	0.25°×0.25°
5	CMCC-ESM2	CMCC	Italy	0.25°×0.25°
6	CanESM5	CCCMA	Canada	0.25°×0.25°
7	MIROC6	MIROC	Japan	0.25°×0.25°
8	MPI-ESM1-2-HR	MPI	Germany	0.25°×0.25°
9	MPI-ESM1-2-LR	MPI	Germany	0.25°×0.25°
10	MRI-ESM2-0	MRI	Japan	0.25°×0.25°
11	NorESM2-LM	NCC	Norway	0.25°×0.25°
12	NorESM2-MM	NCC	Norway	0.25°×0.25°
13	TaiESM1	RCEC	China	0.25°×0.25°

2.3. Methods

2.3.1. Extreme precipitation index

The Intergovernmental Panel on Climate Change (IPCC) delineates extreme weather and climatic phenomena as instances wherein a particular meteorological or climatic variable surpasses (or falls below) a designated threshold, situated proximate to the uppermost (or lowermost) spectrum of its historically observed values [19]. In scientific research applications, meteorologists can quantitatively define extreme climate events. The manuscript delineates a threshold-based extreme climate index, which researchers ubiquitously employ to investigate extreme climatic phenomena. This index's versatility is underscored by its applicability across diverse regions and adaptability to myriad datasets, facilitating nuanced comparative analyses.

Table 2 shows the eight extreme precipitation indices recommended by the Expert Group on Climate Change Detection and Extreme Event Indices (ETCCDI) used in this study [20,21]. These indices can be divided into four categories: one is an absolute index, such as R10. The second is a relative index, such as PRCPTOT, R95p and R99p. The third is an extreme value index, such as RX1day. The fourth is another index, such as CDD, CWD and SDII.

Table 2. Introduction of extreme precipitation indices.

Index	Abbreviation	Definition	Unit
Moderate rainy days	R10	Number of days with daily precipitation ≥ 10mm	d
Total annual precipitation	PRCPTOT	Cumulative precipitation with daily precipitation ≥ 1mm	mm
Heavy precipitation	R95p	Annual cumulative precipitation with daily precipitation > 95% quantile	mm

Preprints (www.preprints.org) | NOT PEER-REVIEWED | Posted: 13 September 2023 doi:10.20944/preprints202309.0809.v1

Very heavy precipitation	R99p	Annual cumulative precipitation with daily precipitation > 99% quantile	mm
1 day maximum precipitation	RX1day	Maximum 1-day precipitation per month	mm
Continuous dry period	CDD	The maximum continuous number of days with daily precipitation < 1mm	d
Continuous wet period	CWD	The maximum continuous number of days with daily precipitation > 1mm	d
Precipitation intensity	SDII	The ratio of total annual precipitation to the number of wet days	$mm \cdot d^{-1}$

2.3.2. RclimDex model

This paper employs the RClimDex model, a computation software grounded in the R language environment, to calculate the extreme climate index. The model conducts a rigorous examination and controls data from the selected stations.We also executed rigorous temporal consistency analyses, eliminating anomalous data points and erroneous values. Advanced measures are implemented, including assessing whether the daily minimum temperature surpasses the established maximum and executing rigorous extreme value analyses [22]. In the rare instances of missing data, we use the linear interpolation method to ensure data integrity and consistency.

The study utilizes daily meteorological data from each station in the Huaihe River Basin and incorporates the precipitation data from the NEX-GDDP-CMIP6 dataset as input for the model. The data from each meteorological station undergoes rigorous correction in a textual format. The data sequence accommodates omissions, designating any absent data with a value of -99.9. During our comprehensive research, we initially scrutinize the meteorological data for logical consistency. Following the completion of this verification phase, we leverage sophisticated computational methodologies to conduct a comprehensive analysis and processing of the data. This meticulous approach ensures the accuracy and reliability of our findings, providing a robust foundation for further scientific inquiries. By standardizing the treatment of missing data, we aim to maintain the integrity of our datasets, facilitating more consistent and meaningful interpretations.

2.3.3. Taylor diagram

The Taylor plot, as introduced by Taylor in 2001, serves as a predominant technique for model evaluation [23]. This method predominantly harnesses three statistical metrics: the correlation coefficient, root mean square error (RMSE) and the standard deviation ratio, facilitating a comprehensive assessment of the congruence or disparity between model simulations and empirical observations.

The Taylor plot critically incorporates the correlation coefficient, quantifying the linear relationship between two datasets. A heightened correlation coefficient underscores a robust linear association between the model simulations and the observed data, denoting enhanced model accuracy. Conversely, the RMSE delineates the variance between the model's projected values and the actual observations. A diminished RMSE value indicates a minimal divergence between the model's forecasts and the observed data, implying heightened model precision.

The standard deviation ratio emerges as a pivotal metric in the Taylor plot. Defined by the quotient of the model's result standard deviation and the observed data's standard deviation, this ratio elucidates the model's variability in juxtaposition with the observed data. When the ratio approximates 1, it signifies a harmonious alignment of the model's variability with the observed data, thereby implying a model of heightened reliability. The graphical representation of the simulated point with the observed datum offers a visual interpretation of the model's simulation prowess. A proximate positioning of the bogus end to the designated marker on the Taylor plot infers a robust simulation capability of the model.

In the context of this paper, both observational data and model data undergo standardization before being evaluated by the Taylor diagram. Standardization is crucial as it enables a fair

 doi:10.20944/preprints202309.0809.v1

comparison between the two sets of data by nullifying the potential influence of differing scales and units. This comprehensive evaluation using the Taylor plot thus aids in verifying the validity and reliability of the model under consideration.

2.3.4. Sen+Mann-Kendall trend analysis

Sen's trend analysis robustly withstands the influence of outliers and operates independently of any specific distribution adherence. It adeptly circumvents measurement inaccuracies and discrete data variances, finding extensive application in climatological and hydrological sequence evaluations [24]. In this paper, the Sen trend is used to analyze the change in the extreme precipitation index in the Huaihe River Basin and the Mann-Kendall method is used to test the significance of the changing trend [25]. The specific calculation formula is as follows:

$$\beta = \text{Median}(\frac{x_j - x_i}{j - i}), \forall j > i \quad (1)$$

In the formula: β is the changing trend of extreme precipitation index, i and j are time series, respectively representing the extreme precipitation index value of the I and jth time. When β>0, the extreme precipitation index is on the rise; β<0 indicates that the extreme precipitation index is on a downward trend.

3. Results

3.1. Taylor Diagram Climate Model Evaluation

Figure 3 comprehensively evaluates the Huaihe River Basin's precipitation patterns from 1960 to 2014, as simulated by 13 global models from the Coupled Model Intercomparison Project Phase 6 (CMIP6). A key metric used in this evaluation is the spatial correlation coefficient, which measures the degree of correlation between the simulated results of these models and the actual observational data gathered within the Huaihe River Basin during the same period. Each of the 13 models demonstrates a spatial correlation coefficient greater than 0.69 and the top five values are all greater than 0.74[26,27]. This strong correlation reflects the models' ability to accurately replicate the spatiotemporal distribution characteristics of precipitation.

The results across the different models are notably consistent, with each demonstrating a similar level of accuracy. This consistency suggests that researchers can reliably use these CMIP6 models to simulate precipitation patterns in the Huaihe River Basin. The Taylor plot evaluation identified the top five performing models as CMCC-CM2-SR5, CMCC-ESM2, TaiESM1, MPI-ESM1-2-LR and CanESM5. We then average these five models to obtain an optimal representation of precipitation in the Huaihe River Basin during the future period.

Preprints (www.preprints.org) | NOT PEER-REVIEWED | Posted: 13 September 2023 doi:10.20944/preprints202309.0809.v1

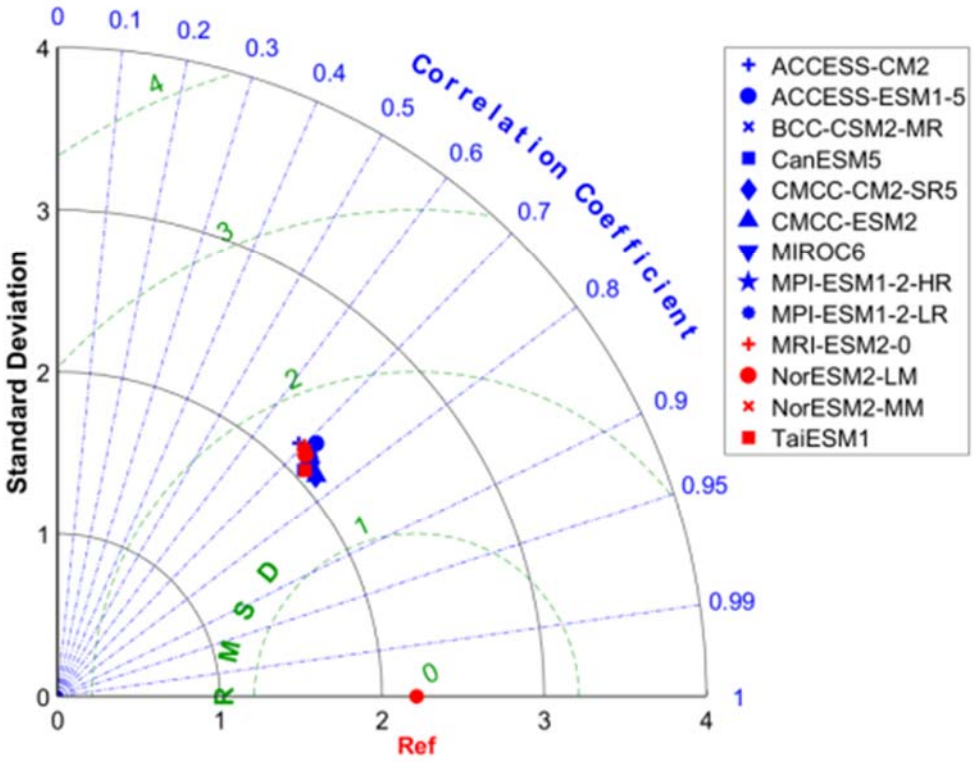

Figure 3. Taylor plots of the average precipitation in the Huaihe River Basin simulated by 13 CMIP6 global models in the historical period (1960-2014).

3.2. Spatiotemporal distribution characteristics of extreme precipitation indices in the Huaihe River Basin in the historical period

3.2.1. Time distribution characteristics of the extreme precipitation index in the Huaihe River Basin in the historical period

The data collected from 1960 to 2014 illustrate the interannual variation trend of the extreme precipitation event index in the Huaihe River Basin, as shown in Figure 4. During these 55 years, several indices of extreme precipitation in the Huaihe River Basin all exhibit an upward trend, including 10mm precipitation days (R10), annual total precipitation (PRCPTOT), extreme precipitation (R95p) and extreme heavy precipitation (R99p). The trend coefficients for these indices are 0.07d/10a, 1.38mm/10a, 5.76mm/10a and 0.32mm/10a. However, these trends do not pass the significance test at a 95% confidence level.

Preprints (www.preprints.org) | NOT PEER-REVIEWED | Posted: 13 September 2023 doi:10.20944/preprints202309.0809.v1

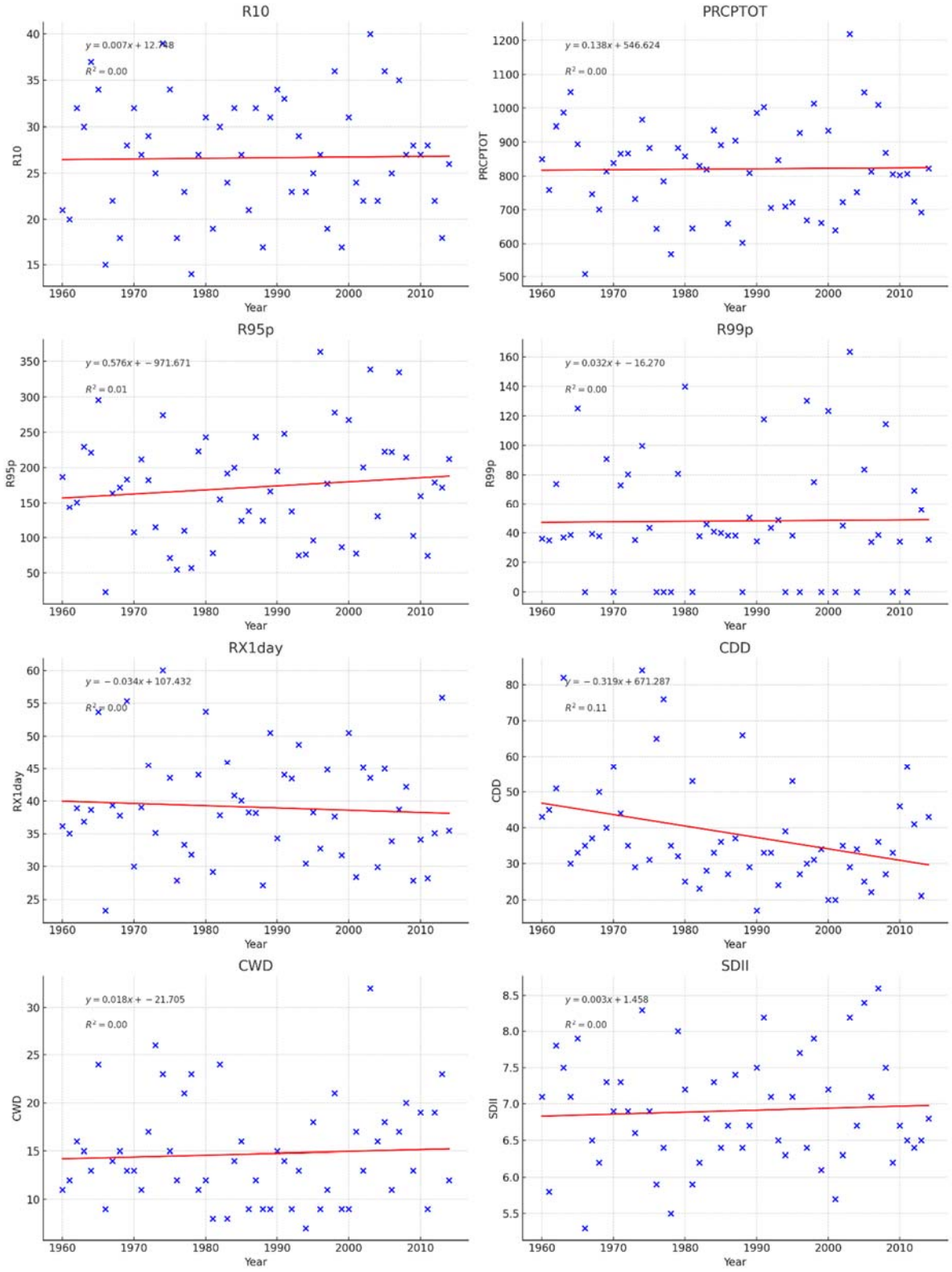

Figure 4. Time distribution characteristics of extreme precipitation index in the Huaihe River Basin in the historical period.

The interannual oscillations of the extreme precipitation event index within the Huaihe River Basin exhibit a nuanced augmentation, though its prominence remains statistically inconsequential. Interestingly, the 1-day maximum precipitation (RX1day) reveals a downward trend with a

Preprints (www.preprints.org) | NOT PEER-REVIEWED | Posted: 13 September 2023 doi:10.20944/preprints202309.0809.v1

coefficient of -0.34mm/10a. However, similar to the upward trend, this trend did not pass the significance test at a 95% confidence level.

On the one hand, the analysis also reveals a downward trend in continuously dry days (CDD) with a -3.19d/10a trend coefficient. In contrast to the other movements, this trend passes the significance test at a 95% confidence level, indicating statistical significance. On the other hand, continuously wet days (CWD) and average daily precipitation intensity (SDII) demonstrate an upward trend. The trend coefficients for these indices were 0.18d/10a and 0.03mm/day/10a. Nonetheless, neither of these trends passed the significance test at the 95% confidence level.

In conclusion, the study of the interannual variation trends of extreme precipitation event indices in the Huaihe River Basin from 1960 to 2014 reveals mixed results. Similarly, while the downward trend in the CDD index is statistically significant, the correlation is low. Further research may be needed to understand the implications of these trends.

3.2.2. Time distribution characteristics of the extreme precipitation index in the Huaihe River Basin in the historical period

Figure 5 shows the spatial distribution of extreme precipitation indices at all monitoring stations from 1960 to 2014. The data encapsulates varying trends in different regions, demonstrating the diversity of climatic conditions across the areas under investigation. One remarkable finding is that except for the Consecutive Dry Days (CDD) index, all other extreme precipitation indices gradually increase as one moves from the northwest towards the southeast. Conversely, CDD gradually decreases as one travels from the northwest to the southeast, suggesting that the northwest more commonly observes dry spells or periods of little to no rainfall than the southeast.

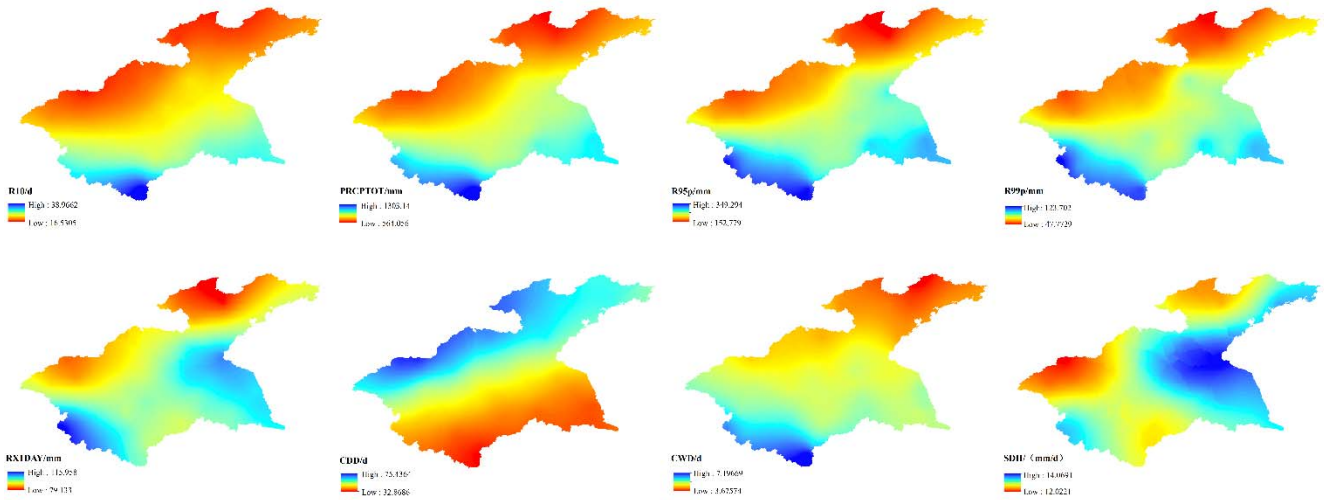

Figure 5. Spatial distribution characteristics of extreme precipitation indices in the Huaihe River Basin in the historical period.

Further analysis reveals that the number of days experiencing precipitation of 10mm or more indicates a slow yet consistent increase from the northwest to the southeast. A peak is observable in the southwest direction of the Huaihe River Basin, suggesting a higher frequency of such rain events in this region. It reaches its zenith in the southwest direction, reflecting an abundance of rainfall conducive to crop cultivation. Moreover, the R95p and R99p indices, representing the total amount of precipitation on days when the amount of rain exceeds the 95th and 99th percentile of a baseline period, respectively, show a rapidly increasing trend from northwest to southeast. However, the R99p index exhibits a faster overall increase compared to R95p. We note their maximum values in the middle and southwestern parts of the Huaihe River Basin, which indicates that this region is more prone to extreme rainfall events.

 doi:10.20944/preprints202309.0809.v1

Interestingly, the daily maximum precipitation follows a similar increasing trend from northwest to southeast. However, its primary distribution is more concentrated in the southeast and southwest of the Huaihe River Basin, suggesting a greater likelihood of intense rainstorms in these areas. Conversely, continuous dry days typically increase from southeast to northwest, showing a clear contrast to the other precipitation indices. The southeast of the Huaihe River Basin has significantly fewer continuous dry days than the northwest, signifying a wetter climate in the south as opposed to drier weather in the north.

It's important to note a significant contrast between the number of continuously wet days and the number of constantly dry days. As we move from the northwest to the southeast, there's an apparent increase in this contrast, which reaches its maximum in the southwest. This pattern suggests that the southwestern region of the Huaihe River Basin has a consistently humid climate throughout the year. Lastly, the average daily precipitation intensity in the Huaihe River Basin generally escalates west to east. While the southwest displays a slightly higher value, the passion remains focused the east. This observation underscores the region's geographic attributes, where rainfall events are typically more intense towards the east.

3.3. Spatiotemporal distribution characteristics of extreme precipitation index in the Huaihe River Basin in the future

3.3.1. Time distribution characteristics of extreme precipitation index in the Huaihe River Basin in the future period

Figure 6 shows the overall characteristics of the changing trends of various indicators in the next 80 years under four different scenarios.In analysing various climate indices, specific patterns emerge across different scenarios. All scenarios exhibit similar distributions for the indices R10, RX1day and SDII, with their median values lying close. SSP3-7.0 and SSP5-8.5 tend to have more comprehensive interquartile ranges in several indices, suggesting more variability. Specifically, SSP3-7.0 consistently shows higher medians in indices related to precipitation extremes such as R95p, R99p and RX1day, indicating anticipation of more severe rain events. SSP1-2.6 often presents tighter distributions, hinting at a potentially more stable or less variable climate in the indices considered.

The SSP3-7.0 and SSP5-8.5 also forecast more consecutive dry days, as the CDD index indicates the possibility of more prolonged dry spells. In contrast, the SSP1-2.6 generally predicts a more consistent climate, as evidenced by its tighter interquartile ranges in several indices. The distributions for CWD across all scenarios are relatively similar, but SSP2-4.5 and SSP3-7.0 show slightly elevated medians. While the medians for some indices across scenarios might appear comparable, the variability, as represented by the interquartile ranges, can be notably different.

It is crucial to contextualise these findings within the broader climate modelling framework. These scenarios are grounded in distinct assumptions about future socio-economic pathways, each with implications for climate change and its subsequent impacts. The observed differences in the indices across the various scenarios are a testament to these underlying assumptions and the diverse potential futures they represent.

Preprints (www.preprints.org) | NOT PEER-REVIEWED | Posted: 13 September 2023 doi:10.20944/preprints202309.0809.v1

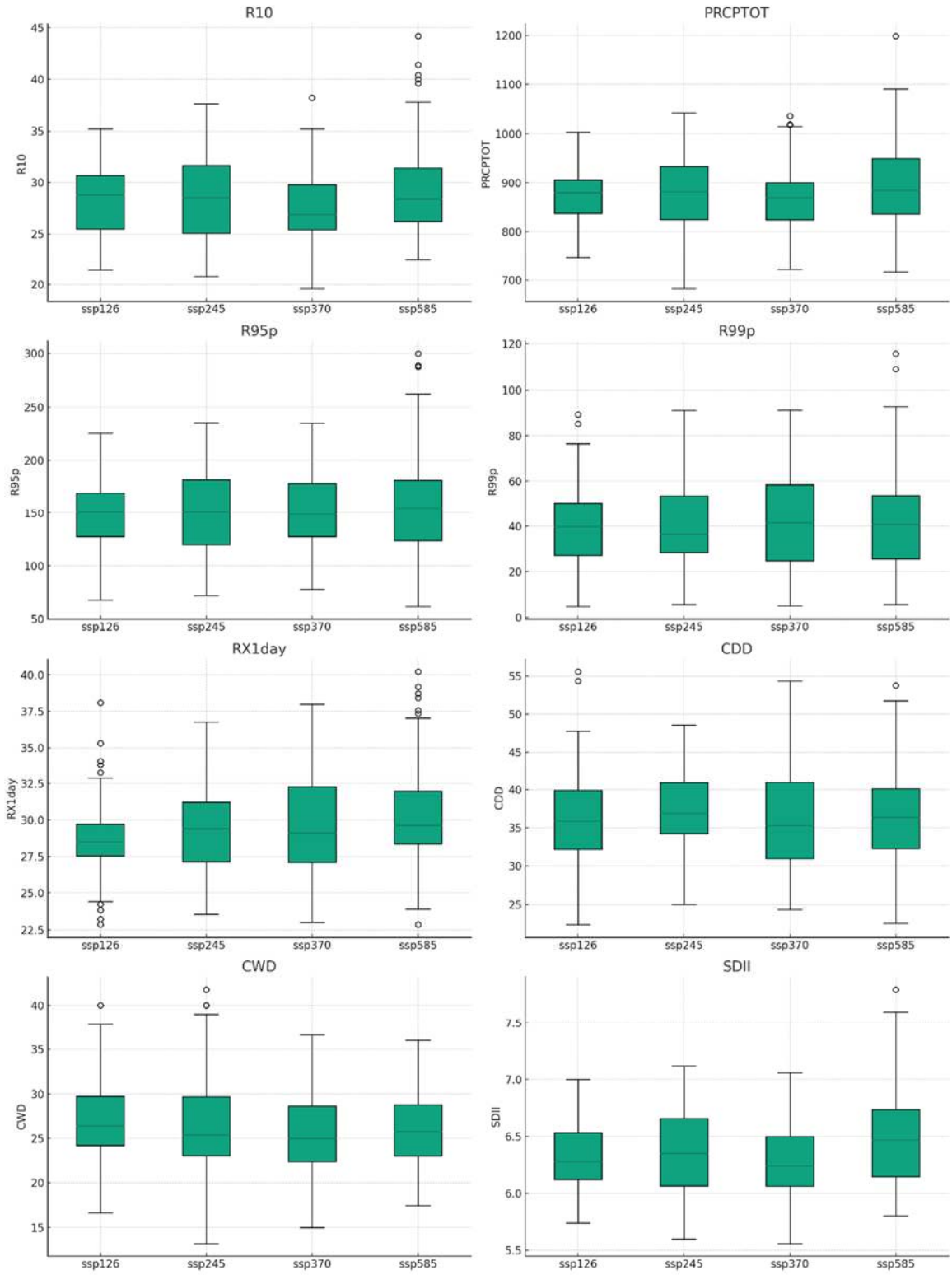

Figure 6. Time distribution characteristics of extreme precipitation index in the Huaihe River Basin in the future period.

3.3.2. Spatial distribution characteristics of extreme precipitation index in the Huaihe River Basin in the future period

It can be seen from Figure 7 that there are significant differences in the variation trends of different extreme precipitation indices from 2021 to 2100. At the same time, a1, a2, a3 and a4 represent the spatial distribution of the relative change rates of each scenario in short-term future (2021-2045).

 doi:10.20944/preprints202309.0809.v1

b1, b2, b3 and b4 represent the mid-term future(2046-2070). c1, c2, c3 and c4 represent the long-term future (2076-2100).

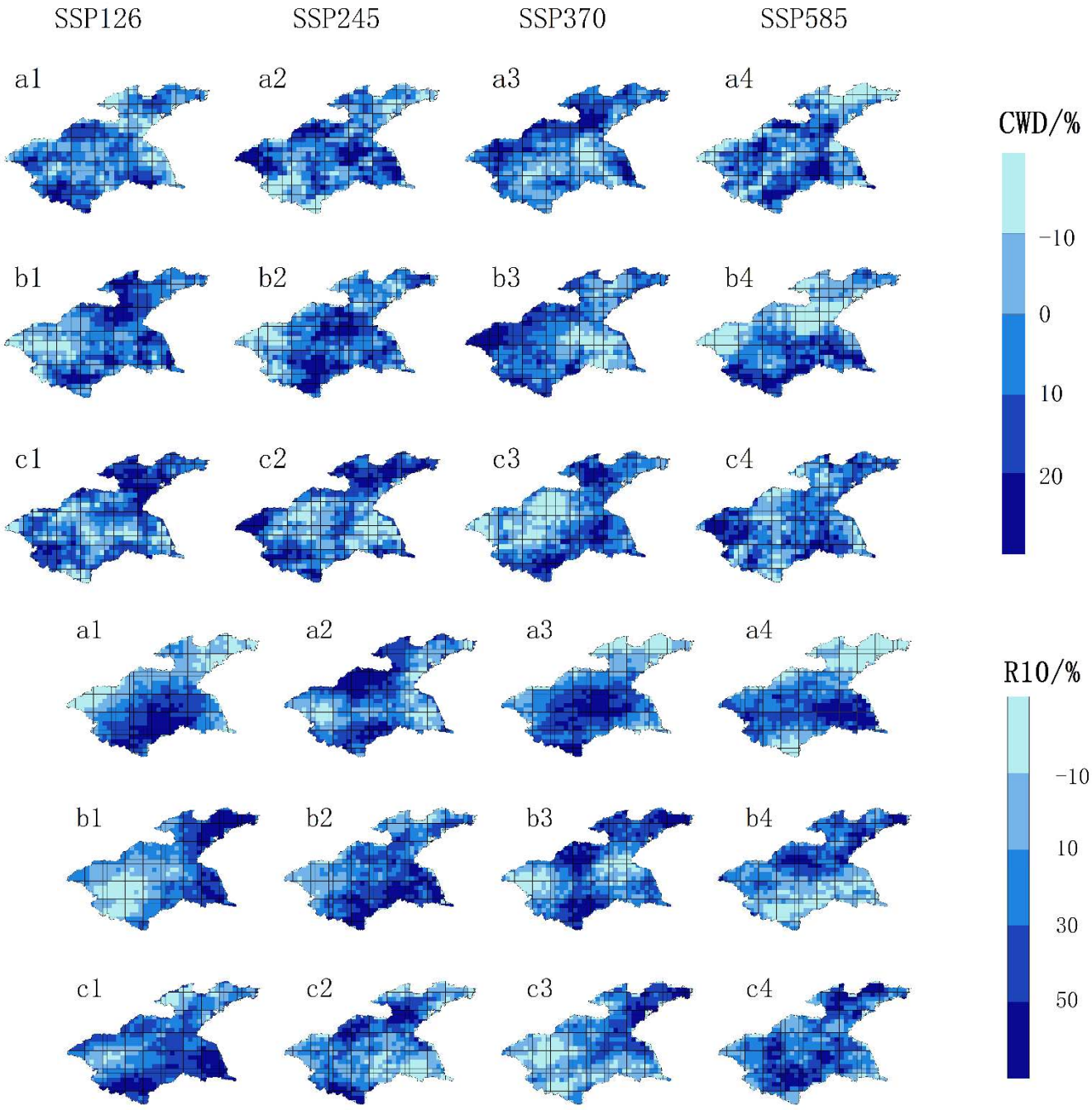

 doi:10.20944/preprints202309.0809.v1

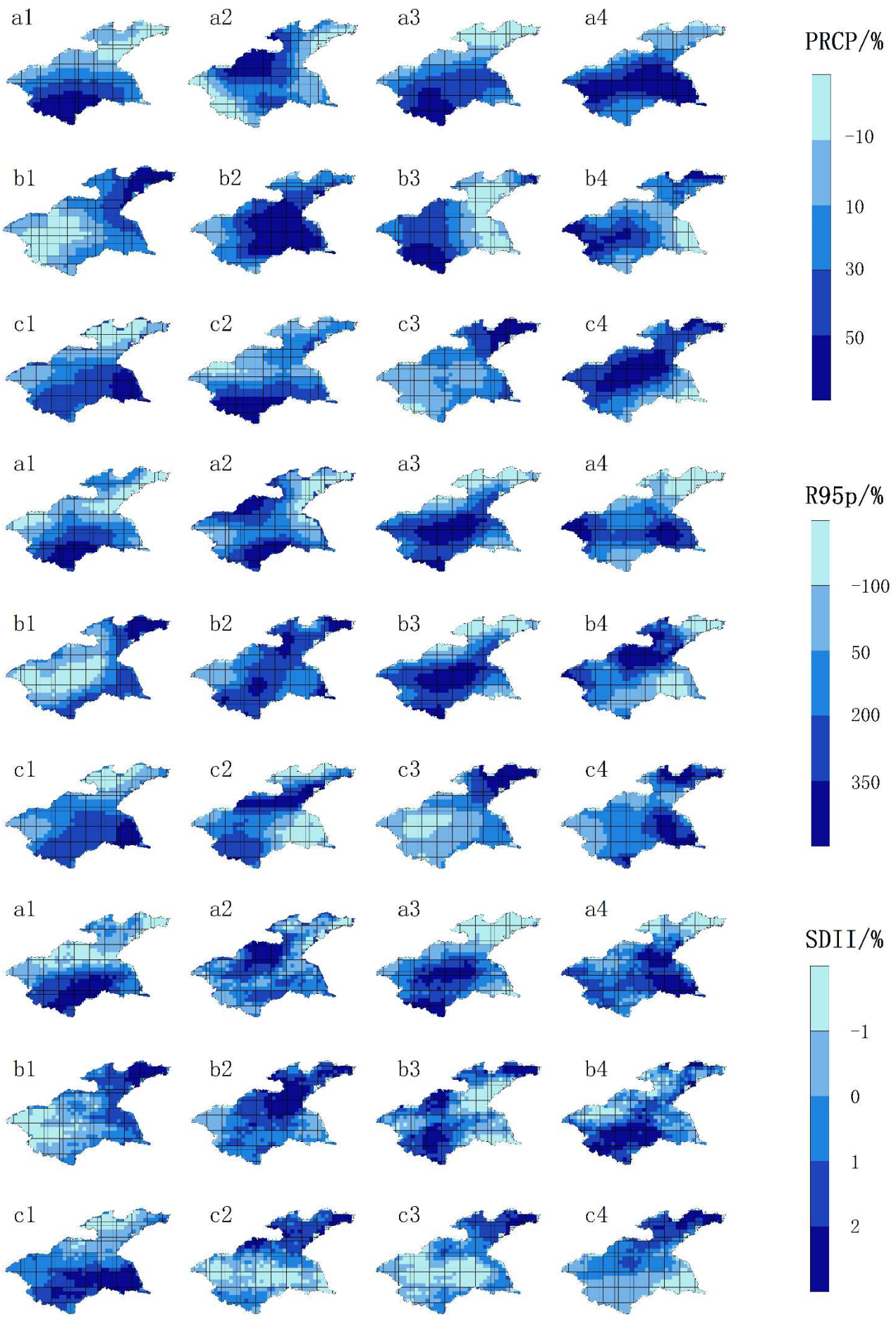

 doi:10.20944/preprints202309.0809.v1

Figure 7. Spatial distribution characteristics of extreme precipitation index in the Huaihe River Basin in the future period.

(1) Short-term future

CWD shows an increasing trend in areas where SSP1-2.6 exceeds 93.6% and SSP3-7.0 exceeds 67.6%, mainly concentrating in the northern and eastern parts of the Huaihe River Basin. However, some places in the central and southern regions are maintaining a decreasing trend. Areas where SSP2-4.5 exceeds 85.9% and SSP5-8.5 surpasses 68.6% also show an increasing trend, mainly concentrating in the middle of the basin, while other regions maintain a steady or decreasing trend.

R10 shows an increasing trend in areas where SSP1-2.6 exceeds 89.8% and SSP3-7.0 exceeds 78.9%. It primarily maintains a rising trend in the central and southern parts of the Huaihe River Basin and a decreasing trend elsewhere. In the scenario of SSP2-4.5, an upwards trend is discernible in over 56.7% of the areas under consideration, with a conspicuous concentration in the north and south, whereas the east and west exhibit a relatively diminished presence. In the scenario of SSP5-8.5, a substantial proportion, specifically exceeding 84.3%, of the regions are exhibiting a growth trend. This expansion primarily manifests in the eastern and western sectors, while it remains noticeably less prevalent in northeast and southwest areas.

PRCPTOT shows an increasing trend in areas where SSP1-2.6 exceeds 95.9% and SSP3-7.0 exceeds 86.4%. The increase is primarily concentrated in the southern part, while other regions show a decreasing trend. Areas where SSP2-4.5 exceeds 86.5%, are also offering an increasing trend. The growth focuses on the northern part of the basin in the middle, while other sites are decreasing. The places where SSP5-8.5 exceeds 87.7% show an increasing trend and the growth area is becoming a horizontal area in the middle of the basin.

R95p is showing an increasing trend in areas where SSP1-2.6 exceeds 87.7% and where SSP3-7.0 exceeds 78.7%, mainly in the southwest of the Huaihe River Basin, while other regions are showing a decreasing trend. The increasing trend in areas where SSP2-4.5 exceeds 56.7% favours more north-south and fewer east-west sites. In contrast, areas where SSP5-8.5 exceeds 85.9%, are revealing a rising trend, with the growing areas concentrating more in the east and west.

SDII shows an increasing trend in areas where SSP2-4.5 exceeds 36.7% and SSP5-8.5 exceeds 90.6%, offering a growing trend in most regions of the Huaihe River Basin. Regions in which the value of SSP1-2.6 surpasses 91.8% are exhibiting an ascending trajectory. The distribution tends to be more in the south and less in the north; the rooms where SSP3-7.0 exceeds 69.7% indicate a growing trend and concentrate in most of the central part of the basin and the southwest region, while the northeast region maintains a decreasing trend.

(2) Mid-term future

CWD shows an increasing trend in areas where SSP1-2.6 exceeds 46.6% and SSP3-7.0 exceeds 58.9%, revealing a distribution state with a significant change rate in the east and west. Areas with SSP5-8.5 exceeding 71.2% show an increasing trend. The distribution state shows a considerable change rate in the north and south. The areas with SSP2-4.5 exceeding 90.5% indicate a growing trend and the places with higher growth rates concentrate in the central and eastern regions of the Huaihe River Basin. In contrast, the change rates in other areas are negative.

R10 shows an increasing trend in areas where SSP1-2.6 exceeds 58.9% and a growing trend in areas where SSP3-7.0 exceeds 73.1%. There is an expanding trend in areas where SSP5-8.5 exceeds 84.5%. The former is rainy in the east and west and the latter is rainy. It is rainy in the north and south. In SSP2-4.5, more than 91.8% of the parts show an increasing trend and all areas except the northwest are rainy.

In SSP1-2.6, PRCPTOT shows an increasing trend in more than 59.7% of the regions. In SSP2-4.5, the whole basin's PRCPTOT offers a growing trend, the east-west distribution is maintained and the total annual precipitation in the east is more than that in the west and central east. In the SSP3-7.0 scenario, there is a noticeable augmentation in the PRCPTOT, an enhancement that permeates more than 79.1% of the assessed regions. In SSP5-8.5, PRCPTOT shows an increasing trend in more than 98.6% of the areas. Under these two scenarios, the total annual precipitation in the basin's west is significantly more than in the east.

 doi:10.20944/preprints202309.0809.v1

In the SSP1-2.6 scenario, there was a noticeable ascending trajectory for the R95p indicator, prevalent in over 57.0% of the regions under consideration. Similarly, within the context of the SSP3-7.0 scenario, this particular metric illustrates an escalating pattern, observable in more than 72.1% of the investigated territories. And the regional distribution is the opposite. The specific performance is that the former offers a less trend in the central area of the basin, while the latter shows an increasing trend in the leading site. In SSP2-4.5, more than 92.1% of the regions showed a rising trend of R95p, mainly showing a growing trend in all areas except the west. The divergence from the R95p model is observed across more than 88.1% of the geographical territories delineated in the SSP5-8.5 scenario, thereby signifying an increasing trend. Remarkably, the northern sectors predominantly localize this amplification.

SDII showed an increasing trend in regions exceeding 40.6% in SSP1-2.6. In SSP2-4.5, SDII is growing in more than 99.3% of the areas. The parts with the highest intensity are all in the northeast of the Huaihe River Basin and other areas of the whole region are higher. In SSP5-8.5, SDII keeps an increasing trend in more than 98.1% of the areas and a rising trend across the entire basin. But in the northwest part, the indicator is decreasing. In SSP3-7.0, more than 92.1% of the regions have increased SDII and they are concentrated in the north and south of the basin, while other areas are relatively flat or reduced.

(3) Long-term future

In SSP1-2.6, SSP2-4.5 and SSP5-8.5, more than 46.7%, 59.8% and 58.3% of the regions show an increasing trend of CWD and they are all in the northeast and southwest parts of the Huaihe River Basin. In SSP3-7.0, more than 65.3% of the regions show an increasing CWD trend, excluding the watershed's northwestern part.

R10 shows an increasing trend in more than 53.9% of the regions in SSP1-2.6. In SSP5-8.5, more than 97.2% of the parts maintain growth. In general, most areas of the Huaihe River Basin show an increasing trend and only a few places in the north and west keep a decreasing trend. In scenario SSP2-4.5, the R10 index increases in more than 87.9% of the regions. It mainly distributes in the north and south and shows a decreasing trend in the central part. In SSP3-7.0, a substantial majority, precisely 90.4% of the regions, are witnessing an ascendant trend. We predominantly observe this upward trajectory in the eastern sectors and other significant areas.

PRCPTOT shows an increasing trend in more than 37.7% of the regions in scenario SSP1-2.6 and more than 91.8% of the areas in SSP2-4.5. All of them are concentrated in the southeast and southern regions, while other parts show a decreasing trend. In SSP3-7.0, PRCPTOT increases in all areas, with the highest increase concentrated in the northeast of the basin. In SSP5-8.5, PRCPTOT also increases in more than 95.7% of the regions and the areas with increasing precipitation become the northern and western basins.

R95p has increased in over 58.3% of the regions in the SSP1-2.6 scenario, showing a decreasing trend from south to north. In SSP2-4.5, around 96.2% of the regions experience growth, primarily in the north and southwestern areas. More than 91.8% of the parts in the SSP3-7.0 scenario show an increase, with growth mainly observed in the northeastern region. In SSP5-8.5, over 99.6% of the areas exhibit an increasing trend, covering the entire Huaihe River Basin.

SDII displays an increasing trend in areas where SSP1-2.6 exceeds 34.8%, with a decreasing trend from south to north. Conversely, in the SSP5-8.5 scenario, the trend is reversed, showing an increasing trend in areas exceeding 98.9% and a decreasing trend from north to south, in regions where SSP2-4.5 and SSP3-7.0 surpass 88.1% and 82.4%, an increasing trend is observed, with growth concentrated in the northern and northeastern areas.

4. Discussion

4.1. Model Evaluation and Historical Analysis

Using the Taylor diagram to evaluate the performance of various climate models is a practical approach widely adopted in climate studies [28]. The high spatial correlation coefficient of over 0.69 across 13 global models from CMIP6 is noteworthy and indicates the reliability of these models in

simulating precipitation patterns. The supplementary literature shows a spatial correlation coefficient 0.69, indicating reasonable accuracy [29]. As a result, the findings strengthen their credibility and align with other studies that have reported high performance of CMIP6 models across various geographical settings [30]. Further bolstering the credibility of the findings is consistency across models. The selection of the top five models with values above 0.74, namely CMCC-CM2-SR5, CMCC-ESM2, TaiESM1, MPI-ESM1-2-LR and CanESM5, provides a robust representation of future predictions. Climate models have been used in the Huaihe River Basin to understand hydrological responses under different scenarios [31].

A comparison of historical data between 1960 and 2014 shows historical trends. While several indices of extreme precipitation exhibit an upward trend, their statistical significance remains inconclusive. The only exception is CDD, which shows a statistically significant downward trend. As a result, extreme rainfall events are occurring more frequently, while dry days are decreasing. There are implications for both agriculture and infrastructure in the Huaihe River Basin due to this complex scenario. On the one hand, increased extreme precipitation can lead to flooding, affecting agriculture and infrastructure. On the other hand, a decrease in dry days might benefit agriculture but could also lead to waterlogging issues.

Using Taylor diagrams and a high spatial correlation coefficient validates the effectiveness and reliability of selected climate models. In the Huaihe River Basin, these models offer valuable insights into precipitation patterns and their potential impacts, which are necessary for future planning and risk management.

4.2. Spatial Variation and Regional Disparities

With its intricate climatic tapestry, the Huaihe River Basin, reveals itself through the spatial distribution of extreme precipitation indices. A discernible increasing trend characterizes most of these indices, transitioning from the northwest to the southeast, except for the CDD. This pattern underscores the heightened vulnerability of the southeastern region to extreme rainfall events, presenting potential challenges and considerations for flood management and agricultural strategies. Conversely, the southwest direction of the basin emerges as a beacon of agricultural promise. The consistent and higher frequency of rain events in this quadrant attests to its natural predisposition for crop cultivation. It emphasizes the region's advantage, fortified by its generous rainfall. This intricate spatial variation underscores the need for region-specific strategies and interventions, ensuring that each area harnesses its climatic strengths while mitigating potential vulnerabilities.

4.3. Future Projections and Implications

The projections spanning from 2015 to 2100 hold profound significance. Analyzing various scenarios, such as SSP1-2.6, SSP2-4.5, SSP3-7.0 and SSP5-8.5, provides a comprehensive understanding of potential future trends. The evidence indicates a potential intensification of rainfall events within the Huaihe River Basin, most notably within the parameters of the SSP3-7.0 scenario, thereby influencing the region's strategic approaches to flood management, infrastructural advancements and agronomic methodologies.

Furthermore, the future distribution characteristics of precipitation patterns demonstrate regional disparities. The upward trajectory of indices such as CWD, R10, PRCPTOT, R95p and SDII in the basin's northeastern, southwestern and southeastern sectors intimates a potential intensification of precipitation and protracted wet durations in these locales. Such a climatic shift presents a dichotomy of outcomes: on the one hand, augmented rainfall augurs well for agricultural endeavours, yet on the other, it precipitates complexities in water stewardship, flood mitigation and infrastructural resilience.

5. Conclusions

Utilizing observational data from 45 meteorological stations situated in the Huaihe River Basin spanning the period from 1960 to 2014, in conjunction with the NEX-GDDP-CMIP6 precipitation

model dataset, we conduct a comprehensive analysis of the spatiotemporal variation attributes of the extreme precipitation index for both historical and projected future intervals, employing sophisticated methodologies including the Taylor diagram and trend analysis techniques. The main conclusions are as follows:

(1) Over the past 55 years, the interannual variation trend of the extreme precipitation event index in the Huaihe River Basin has yet to be apparent. There is only a slight but statistically insignificant increase. Spatially, except for CDD, the extreme precipitation indices show a gradual increase from northwest to southeast, while CDD exhibits a decreasing trend from northwest to southeast.

(2) Under the same scenario in the future, the rate of change of each index will continue to increase over time. Spatially, the future increase in extreme precipitation in the Huaihe River Basin will exhibit a spatial variation characteristic that decreases from northwest to southeast. With the evolution of different scenarios, we anticipate a gradual escalation in the annual and excessive precipitation growth rates. Moreover, as time unfolds, the disparity between these varied scenarios is expected to amplify significantly. Additionally, the intensity of extreme precipitation may increase in the southeast of the Huaihe River Basin.

(3) CWD, R10mm, PRCPTOT, R95p and SDII are the leading indices that affect extreme precipitation changes in the Huaihe River Basin. Judging from the performance of these indicators on the map, the northeast, southwest and southeastern parts of the Huaihe River Basin will experience more precipitation and longer wet periods for most of the forecasted next 80 years. In other regions, the rainfall situation will vary significantly in different periods.

Author Contributions: : Conceptualization, data collection, formal analysis, writing—original draft preparation: Min Tong; writing—review and editing, supervision: Leilei Li. All authors have read and agreed to the published version of the manuscript.

Funding: This research was funded by the fund of Henan Province Fund (Research on flood risk information technology) [Grant No. 232102320002] and the National Natural Science Foundation of China (Grant No. 42101383).

Data Availability Statement: The data that support the findings of this study are available from the corresponding author upon reasonable request. Some data are not publicly available due to privacy or ethical restrictions. The data that are publicly available can be found in the NCCS (https://www.nccs.nasa.gov/services/data-collections/land-based-products/nex-gddp-cmip6) and Google Scholar (https://scholar.google.com.hk/?hl=en).

Acknowledgments: We want to express our deepest gratitude to the faculty and staff of the School of Earth Science and Technology, Zhengzhou University, for their invaluable guidance and support throughout the research process. Special thanks to the academic team for their tireless efforts to ensure the smooth progress of the project from the initial proposal stage to the final paper submission. We also thank Dr. Leilei Li for technical support, whose expertise was instrumental during this study's data collection and analysis phases. In addition, we would also like to thank the fund of Henan Province Fund for their generous donation of materials and resources, which significantly contributed to the successful completion of our experiments. Lastly, we express our gratitude to peers and colleagues who provided constructive feedback and moral support during the research process.

Conflicts of Interest: The authors declare no conflict of interest.

References

1. Adopted, I. P. C. C. (2014). Climate change 2014 synthesis report. IPCC: Geneva, Szwitzerland, 1059-1072.
2. Xu, D., Liu, D., Yan, Z., Ren, S., & Xu, Q. (2023). Spatiotemporal variation characteristics of precipitation in the Huaihe River Basin, China, as a result of climate change. Water, 15(1), 181.
3. Lin, H., Wang, J., Li, F., Xie, Y., Jiang, C., & Sun, L. (2020). Drought trends and the extreme drought frequency and characteristics under climate change based on SPI and HI in the upper and middle reaches of the Huai River Basin, China. Water, 12(4), 1100.
4. Khaing, Z. M., Zhang, K., Sawano, H., Shrestha, B. B., Sayama, T., & Nakamura, K. (2019). Flood hazard mapping and assessment in data-scarce Nyaungdon area, Myanmar. PLoS One, 14(11), e0224558.

5. Wang, G., Zhang, Q., Yu, H., Shen, Z., & Sun, P. (2020). Double increase in precipitation extremes across China in a 1.5° C/2.0° C warmer climate. Science of the Total Environment, 746, 140807.
6. Allan, R. P., & Soden, B. J. (2008). Atmospheric warming and the amplification of precipitation extremes. Science, 321(5895), 1481-1484.
7. Yazdandoost, F., Moradian, S., Izadi, A., & Aghakouchak, A. (2021). Evaluation of CMIP6 precipitation simulations across different climatic zones: Uncertainty and model intercomparison. Atmospheric Research, 250, 105369.
8. Masson-Delmotte, V., Zhai, P., Pirani, A., Connors, S. L., Péan, C., Berger, S., ... & Zhou, B. (2021). Climate change 2021: the physical science basis. Contribution of working group I to the sixth assessment report of the intergovernmental panel on climate change, 2.
9. Yao, Y., Qu, W., Lu, J., Cheng, H., Pang, Z., Lei, T., & Tan, Y. (2021). Responses of hydrological processes under different shared socioeconomic pathway scenarios in the Huaihe River Basin, China. Water, 13(8), 1053.
10. Xu Feng, & Niu Jiqiang. (2004). Flood disasters and countermeasures in the Huaihe River Basin. Journal of Xuchang University, 23(5), 105-109.
11. Bi Baogui, Jiao Meiyan, & Li Zechun. (2004). Meteorological and hydrological characteristics of floods and rainstorms in the Huaihe River Basin in 2003. Journal of Nanjing Meteorological Institute, 27(5), 577-586.
12. Jiao Meiyan, Jin Ronghua, & Qi Dan. (2008). Meteorological and hydrological characteristics of Huaihe River rainstorm and flood in 2007. Journal of Applied Meteorology, 19(3), 257-264.
13. Nashwan, M. S., & Shahid, S. (2020). A novel framework for selecting general circulation models based on the spatial patterns of climate. International Journal of Climatology, 40(10), 4422-4443.
14. Huang Xiaoyuan, & Li Xiehui. (2022). Future prediction of rainstorm and flood disaster risk in southwest China based on CMIP6. Journal of Applied Meteorology, 33(2), 231-243.
15. Feng Yelin, He Zhonghua, Jiao Shulin & Liu Wei. (2023). Prediction of extreme precipitation scenarios in Guizhou Province based on CMIP6 climate model. Soil and Water Conservation Research(01),282-290.
16. Dewan, A. M., Corner, R., Hashizume, M., & Ongee, E. T. (2013). Typhoid fever and its association with environmental factors in the Dhaka metropolitan area of Bangladesh: a spatial and time-series approach. PLoS neglected tropical diseases, 7(1), e1998.
17. Minh, P. T., Tuyet, B. T., & Thao, T. T. T. (2018). Application of ensemble Kalman filter in WRF model to forecast rainfall on monsoon onset period in South Vietnam. Vietnam Journal of Earth Sciences, 40(4), 367-394.
18. Zhang, Q., Li, J., Singh, V. P., & Xu, C. Y. (2013). Copula-based spatio-temporal patterns of precipitation extremes in China. international Journal of Climatology, 33(5), 1140-1152.
19. Field, C. B. (Ed.). (2012). Managing the risks of extreme events and disasters to advance climate change adaptation: special report of the intergovernmental panel on climate change. Cambridge University Press.
20. Ma Jianing, & Gao Yanhong. (2019). Analysis of annual average and extreme precipitation changes in the upper reaches of the Yellow River in the past 50 years. Plateau Meteorology, (1), 124-135.
21. Jin Ruimeng, & Yang Yang. Evaluation of the CMIP5 global climate model for the simulation of the northward extension of rain belts in eastern China. Meteorological Hydro-Oceanic Instruments, 39(3), 19-23, 2022.
22. Wang Qiong, Zhang Mingjun, Wang Shengjie, Luo Shufei, Wang Baolong, & Zhu Xiaofan. (2013). Analysis of extreme temperature events in the Yangtze River Basin from 1962 to 2011. Acta Geographica Sinica, 68(5), 611-625.
23. Taylor, K. E. (2001). Summarizing multiple aspects of model performance in a single diagram. Journal of geophysical research: atmospheres, 106(D7), 7183-7192.
24. Liu Xianfeng, Hu Baoyi, & Ren Zhiyuan. (2018). Temporal and spatial changes and driving factors of water use efficiency of vegetation ecosystems on the Loess Plateau. Chinese Agricultural Sciences, 51(2), 302-314.
25. Li Shuangshuang, Yang Saini, & Liu Xianfeng. (2015). Spatiotemporal variation characteristics and influencing factors of extreme precipitation in the north and south of Qinling-Huaihe River from 1960 to 2013. Advances in Geographical Sciences, (3), 354-363.
26. Wang, D., Liu, J., Wang, H., Shao, W., Mei, C., & Ding, X. (2022). Performance evaluations of CMIP6 and CMIP5 models for precipitation simulation over the Hanjiang River Basin, China. Journal of Water and Climate Change, 13(5), 2089-2106.

27. Xu, D., Liu, D., Yan, Z., Ren, S., & Xu, Q. (2023). Spatiotemporal variation characteristics of precipitation in the Huaihe River Basin, China, as a result of climate change. Water, 15(1), 181.
28. Ngoma, H., Wen, W., Ayugi, B., Babaousmail, H., Karim, R., & Ongoma, V. (2021). Evaluation of precipitation simulations in CMIP6 models over Uganda. International Journal of Climatology, 41(9), 4743-4768.
29. Pan, H., Jin, Y., & Zhu, X. (2022). Comparison of projections of precipitation over Yangtze River Basin of China by different climate models. Water, 14(12), 1888.
30. Pomee, M. S., & Hertig, E. (2022). Precipitation projections over the Indus River Basin of Pakistan for the 21st century using a statistical downscaling framework. International Journal of Climatology, 42(1), 289-314.
31. Yao, Y., Qu, W., Lu, J., Cheng, H., Pang, Z., Lei, T., & Tan, Y. (2021). Responses of hydrological processes under different shared socioeconomic pathway scenarios in the Huaihe River Basin, China. Water, 13(8), 1053.